Phase Behavior of a DNA-Based Surfactant Mixed with Water and *n*-Alcohols

Cecilia Leal,* Azat Bilalov,† and Björn Lindman

Physical Chemistry 1, Center of Chemistry and Chemical Engineering, University of Lund, POB 124, Lund 22100, Sweden

Received: April 6, 2006; In Final Form: July 10, 2006

The self-assembly behavior of a cationic surfactant (dodecyltrimethylammonium, DTA) with DNA as counterion in mixtures of water and *n*-alcohols (decanol, octanol, hexanol, butanol, and ethanol) was investigated. The phase diagrams were established and the different regions of the phase diagram characterized with respect to microstructure by ^{2}H NMR, small-angle X-ray scattering (SAXS), and other techniques. The DNA−DTA surfactant is soluble in all of the studied alcohols, showing increased solubility from decanol down to ethanol. All of the phase diagrams are analogous with respect to the occurrence of liquid crystalline (LC) regions, but the area of the LC region increases as one goes from decanol to ethanol. In all phase diagrams, hexagonal phases (of the reversed type) for the alcohol-rich side and lamellar phases for the other side were detected. For balanced proportions of the components, there is a coexistence of the lamellar and the hexagonal phase, here detected with a double quadrupole splitting in the ^{2}H NMR spectra. The correctness of the phase diagrams is confirmed by the fact that along the tie-lines the splitting magnitude remains nearly constant. All of the alcohols except for ethanol act as cosurfactants penetrating the DNA−DTA film. Adding salt to the ternary mixtures causes an increase in the unit cell dimension of the lamellar and the hexagonal phases. The phase diagram becomes more complicated when butanol is used for the alcohol phase. Here, there is the occurrence of a new isotropic phase with some properties analogous to those of the disordered sponge (L3) phase obtained for simple surfactant systems.

Introduction

Polyelectrolyte−surfactant complexes represent a class of materials formed noncovalently by self-assembly, and possessing nanoscopic order. These materials often exhibit a rich phase behavior, and, by changing temperature, charge density, hydrophobic content, etc., polyelectrolyte−surfactant complexes can be tailored to better realize certain macroscopic properties. In addition to the fundamental interest in the principles governing phase behavior, aggregation, and precipitation of polyelectrolyte−surfactant mixtures, understanding the behavior of these complex systems is crucial for technological applications concerning detergents, paints, shampoos, cosmetics, and others.[1−10] When biopolymers such as DNA or proteins are associated with surfactants, then novel biotechnological applications such as DNA protection and purification, drug, and nonviral gene delivery become possible.[11−18] In vivo and in vitro processes regarding DNA usually involve DNA association with other species via electrostatic or/and hydrophobic interactions. The compaction of DNA by surfactants becomes important because associations both by charge and by hydrophobic effects play a role. Analogously to classic polyelectrolyte−surfactant aggregates, the phase behavior can be perturbed also in DNA−surfactant complexes by changing certain conditions. One example is the formation of a reversed hexagonal phase by incorporation of a reasonably long chain alcohol[14] in a lamellar phase comprising lipids and DNA. This behavior is also observed when the lipid is substituted by a single chain ionic surfactant molecule.[19] The main mechanisms involved in the complexation of highly charged semi-flexible polyelectrolytes and oppositely charged surfactants are electrostatic attraction and counterion release.[20] A system of polyelectrolyte, oppositely charged surfactant, and water, normally a four-component system, can be simplified and treated as a three-component system if a complex salt is prepared.[8] A complex salt is a stoichiometric aggregate where every charge in the polyelectrolyte is compensated by the surfactant in such a way that an electroneutral complex is formed, with essentially all counterions eliminated.[20] With this approach, one obtains true ternary mixtures, the phase behavior of which can be more easily investigated and can be represented in two dimensions (at constant temperature and pressure).

The resulting material of a combination between DNA and surfactants possesses distinct properties including insolubility in water but solubility in some hydrophobic solvents,[21] nonredissolution in the presence of excess of surfactant,[22] among many others. Interestingly, it also shows many similarities to the components alone. In terms of supramolecular arrangement, the complexes formed resemble those of the surfactants[13,23,24] or DNA at high concentration.[25] With respect to miscibility, we have found interesting similarities to the classical surfactant emulsification of oils and water when a DNA-based surfactant is used.[19] Decanol and water could be mixed by a cationic surfactant where its bromide counterion was replaced by DNA. The homogeneous phase was liquid crystalline rather than a microemulsion classically obtained with simple surfactants due to the high rigidity of the DNA−surfactant films. In this paper, we extend the characteristics obtained for the DNA−DTA/decanol/water mixture to a series of lower alcohols.

Materials and Methods

Materials. Na-deoxyribonucleic acid sodium salt from Herring testes (Sigma) was used as received. Herring testes DNA

* Corresponding author. E-mail: cecilia.leal@fkem1.lu.se.
† On leave from Physical and Colloid Chemistry, Kazan State Technological University, Russia.

10.1021/jp062151f CCC: $33.50
Published on Web 08/08/2006

is highly polydisperse with an average molar mass of 700 bp, determined by electrophoresis. The concentration of DNA was determined by UV methods. The A_{260}/A_{280} ratio of DNA solutions was found to be 1.8, suggesting that DNA was free of proteins.[26] Sodium bromide (Riedel-deHaen extra pure quality) was used as received. Dodecyltrimethylammonium bromide (DTAB) was obtained from Tokyo Kasei Kogyo Co., Ltd., and used without further purification. Organic solvents (decan-1-ol, octan-1-ol, hexan-1-ol, butan-1-ol, ethanol), especially pure, BDH Chemicals Ltd., were used as received. Sodium chloride (NaCl) was obtained from Sigma. The water used was from a Milli-Q filtration system (Millipore). D_2O was obtained from Dr. Glaser AG, Basel.

Preparation of the Complex Salt DNA−DTA. DNA solutions were prepared by weighing the desired amount and dissolving it in 10 mM NaBr. The pH of all solutions was 7 ± 0.2. Stoichiometric DNA−surfactant aggregates were prepared my mixing equal amounts of moles of negative charges of DNA and positive charges of DTA (200 mL of 5 mM solutions) under stirring. Under these conditions, the counterion release should be maximal and nearly complete.[20] The precipitate was equilibrated in solution for 48 h. It was then separated from the aqueous phase by filtration and washed extensively with Millipore water. The macromolecular complex salt (DNA−DTA) was dried for 3 days in a DW6-85 freeze-dryer.

Sample Preparation. Appropriate amounts of the DNA−DTA complex, *n*-alcohol, and water (for the NMR experiments, heavy water was used) were weighed into 8 mm (i.d.) glass tubes, which were flame-sealed immediately. First, the components were mixed with a Vortex vibrator; next, the mixing was continued in a centrifuge over a few days at 4000 rpm and 40 °C. The tubes were turned end over end every 15 min. The samples were left to equilibrate in a temperature-controlled room at 25 ± 0.5 °C for 2−6 months.

Methods. The samples were investigated by visual inspection in normal light and between crossed polarizers in polarized light to detect anisotropic (birefringent) and isotropic (nonbirefringent) phases, as well as to distinguish between one-phase (transparent) and two-phase (nontransparent) regions. The more detailed structural investigation was obtained with ^{2}H NMR and small-angle X-ray scattering (SAXS).

^{2}H NMR (D_2O). The ^{2}H NMR spectrum from deuterated water is dominated by the interaction of the deuteron electric quadrupole moment with the electric field gradients at the nucleus. The anisotropy of liquid crystalline (LC) samples prevents the quadrupole interaction from averaging to zero, giving rise to a NMR spectrum with two peaks of equal intensity (quadrupole splitting). For an isotropic LC phase, or a solution, a single sharp peak is obtained because of isotropic molecular motions, which average the interactions to zero.[27] The magnitude of the splitting obtained from ^{2}H NMR depends, among other things, on the angle θ between the axis of cylindrical symmetry (director) and the magnetic field as well as the fraction of bound ^2H_2O in one or more anisotropic sites.[28] For a system containing more than one phase, the ^{2}H NMR spectra are superimposed unless there is fast ^{2}H exchange between the phases. For a mixture of hexagonal and lamellar liquid crystalline phases, two splittings can then be observed with the one originating from the lamellar phase being ideally twice the magnitude of that obtained for the hexagonal phase.[29] The experiments were performed at a frequency of 15.371 MHz on a Bruker DMX 100 spectrometer equipped with a 100 MHz (2.3 T) wide-bore superconducting magnet. The temperature was controlled with an airflow through the sample holder.

Small-Angle X-ray Scattering (SAXS). The measurements were performed on a Kratky compact small-angle system equipped with a position sensitive detector (OED 50M from M Braun, Graz, Austria) containing 1024 channels with 53.0-μm width. Cu Kα radiation of wavelength 1.542 Å was provided by a Seifert ID300 X-ray generator operating at 50 kV and 40 mA. A 10 μm thick nickel filter was used to remove the Kβ radiation, and a 1.55-mm tungsten filter was used to protect the detector from the primary beam. The sample-to-detector distance was 277 mm. The volume between the sample and the detector was kept under vacuum during data collection to minimize the background scattering. The temperature was kept constant at 25 °C (±0.1 °C) with a Peltier element.

Results and Discussion

General Outline of Phase Diagrams. Our first comprehensive data on a DNA−DTA/alcohol/water system were described previously[19] by using decanol as an oil phase. The term "oil phase" regards the low polarity solvent decanol with a finite water content. More than 150 samples were equilibrated for 2 months, and some of them were rechecked after 6 months. Here, we provide a general outline of the phase diagrams obtained for lower alcohols (octanol, hexanol, butanol, and ethanol) based on 50 samples per diagram with exception to the DNA−DTA/butanol/water system where more than 100 samples were used. For the butanol case, notorious differences relative to the higher alcohols start to appear. The differences could be attributed to the partition of the alcohols between the different phases; for instance, the solubility of butanol in water (8.03 wt %) is 10 times higher than that of hexanol (0.7 wt %).[30,31]

The phase diagrams of the ternary system DNA−DTA/*n*-alcohol/water at 25 °C are presented in Figure 1. Sample compositions are given in weight percent of the components. First, the samples were investigated visually in normal light and between cross polarizers to detect anisotropic phases. The samples were then studied via ^{2}H NMR, and it was established whether a certain sample consisted of a single homogeneous phase, two phases, or three phases. The structure of the various phases was investigated via ^{2}H NMR and SAXS.

The phase diagrams obtained for octanol and hexanol are very similar to the one obtained previously for decanol.[19] There are basically eight significant phase regions in the phase diagrams: (1) one-phase region, isotropic alcohol solution (I_1); (2) two-phase region, I_1 + hexagonal liquid crystalline phase (H); (3) three-phase region, aqueous solution with small amounts of dissolved alcohol (I_2) + H + I_1; (4) two-phase regions, (a) I_2 + H and (b) I_2 + lamellar liquid crystalline phase (L); (5) three-phase region, I_2 + L + DNA−DTA complex with a small amount of adsorbed water and alcohol (DNA−DTA); (6) two-phase region, L + DNA−DTA; (7) one-phase regions, (a) H and (b) L; (8) H + L. The phase diagrams with butanol and ethanol appear to be more complicated when compared to the other alcohols. In fact, after 3 months of equilibration, we could still find 24 different regions in the phase diagram of DNA−DTA/butanol/water at 25 °C. We will discuss in detail some of these regions. Nevertheless, a summary of the different phase areas encountered is provided: (1) one-phase region, isotropic butanolic solution (I_1); (2) one-phase region, hexagonal liquid crystalline phase (H); (3) two-phase region, I_1 + H; (4) two-phase region, aqueous solution with lower than 8 wt % of butanol (I_2) + I_1; (5) three-phase region, H + isotropic solution with flow birefringence (S) + I_1; (6) three-phase region, I_1 + S + I_2; (7) two-phase region, H + S; (8) one-phase region, S; (9) two-phase region, I_2 + S; (10) three-phase region, I_2+ H + S;

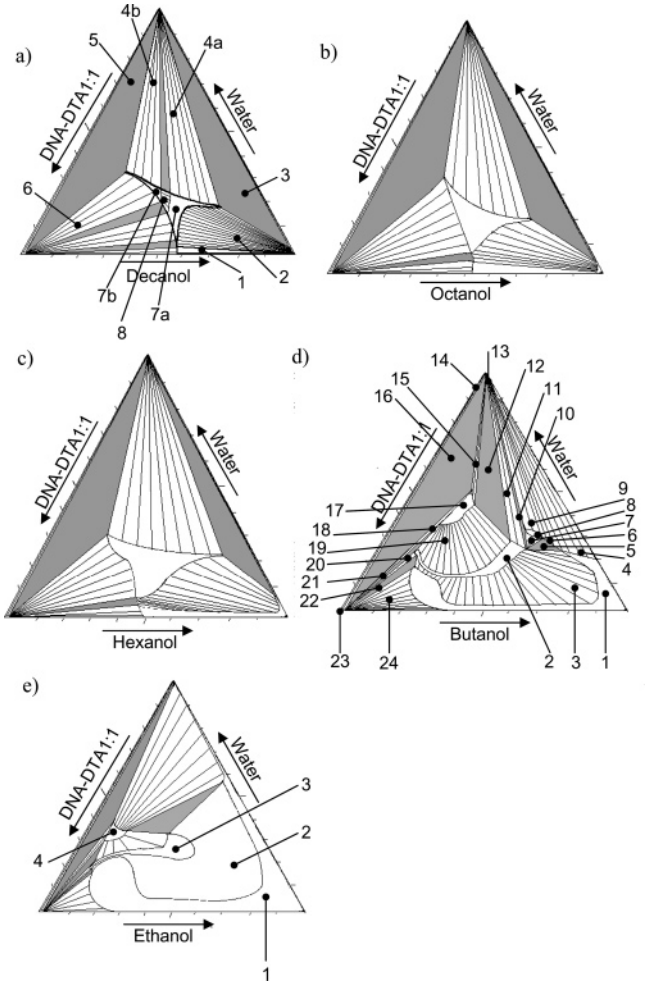

Figure 1. Phase diagrams of the DNA−DTA (1:1) complex/*n*-alcohol/water system at 25 °C. (a) Decanol, (b) octanol, (c) hexanol, (d) butanol, and (e) ethanol. (a−c) (1) One-phase region, isotropic alcohol solution (I_1); (2) two-phase region, I_1 + hexagonal liquid crystalline phase (H); (3) three-phase region, aqueous solution with small amounts of dissolved alcohol (I_2) + H + I_1; (4) two-phase regions, (a) I_2 + H and (b) I_2 + lamellar liquid crystalline phase (L); (5) three-phase region, I_2 + L + DNA−DTA complex with a small amount of adsorbed water and alcohol (DNA−DTA); (6) two-phase region: L + DNA−DTA; (7) one-phase regions, (a) H and (b) L; (8) H + L. (d) (1) One-phase region, isotropic butanolic solution (I_1); (2) one-phase region, hexagonal liquid crystalline phase (H); (3) two-phase region, I_1 + H; (4) two-phase region, aqueous solution with lower than 8 wt % of butanol (I_2) + I_1; (5) three-phase region, H + isotropic solution with flow birefringence (S) + I_1; (6) three-phase region, I_1 + S + I_2; (7) two-phase region, H + S; (8) one-phase region, S; (9) two-phase region, I_2 + S; (10) three-phase region, I_2 + H + S; (11) two-phase region, I_2 + H; (12) three-phase region, I_2 + H + lamellar liquid crystalline phase (L); (13) one-phase region, I_2; (14) two-phase region, I_2 + DNA−DTA; (15) two-phase region, I_2 + L; (16) three-phase region, DNA−DTA + L + I_2; (17) one-phase region, L; (18) two-phase region, L + DNA−DTA; (19) two-phase region, L + H; (20) two-phase region, DNA−DTA + H; (21) three-phase region, DNA−DTA + H + L; (22) three-phase region, DNA−DTA + H + I_1; (23) one-phase region, DNA−DTA; (24) two-phase region, DNA−DTA + I_1. (e) (1) One-phase region, isotropic ethanolic solution (I_1); (2) two-phase region, lower hexagonal liquid crystalline phase (H) + upper I_1; (3) one-phase region, H; (4) one-phase region, lamellar liquid crystalline phase (L).

(11) two-phase region, I_2 + H; (12) three-phase region, I_2 + H + lamellar liquid crystalline phase (L); (13) one-phase region, I_2; (14) two-phase region, I_2 + DNA−DTA; (15) two-phase region, I_2 + L; (16) three-phase region, DNA−DTA + L + I_2; (17) one-phase region, L; (18) two-phase region, L + DNA−DTA; (19) two-phase region, L + H; (20) two-phase region, DNA−DTA + H; (21) three-phase region, DNA−DTA + H + L; (22) three-phase region, DNA−DTA + H + I_1; (23) one-phase region, DNA−DTA; (24) two-phase region, DNA−DTA + I_1.

The DNA−DTA/ethanol/water phase diagram was only partially investigated, and four different regions were encountered: (1) one-phase region, isotropic ethanolic solution (I_1); (2) two-phase region, lower hexagonal liquid crystalline phase (H) + upper I_1; (3) one-phase region, H; (4) one-phase region, lamellar liquid crystalline phase (L).

Isotropic Phase Region (Area 1 in All Phase Diagrams). In the alcohol-rich corner of the phase diagram (area 1 in all phase diagrams), the solutions are transparent, nonbirefringent, and strongly adhesive. The solutions are highly viscous for high contents of the DNA−DTA complex and show rubber-like mechanical behavior.

The area for the isotropic solution of DNA−DTA and *n*-alcohol is larger the shorter is the alcohol. This observation is related to the solubility limit of the DNA−DTA complex and water in the different alcohols. Water solubility in decanol is 3 wt %, while in butanol it is 20 wt %.[30,31] DNA−DTA is soluble in decanol up to 43 wt %. In butanol, the DNA−DTA solubility limit is 65 wt %, and, in ethanol, more than 70 wt % of complex can be solubilized. The DNA−DTA complex is virtually insoluble in water. Several solubility studies indicate that it is possible to solubilize DNA−surfactant complexes in a number of low-polarity organic solvents.[21,32] It has also been demonstrated that alcohol is a good solvent for DNA−surfactant complexes, and this was attributed to micelle destabilization.[33] In simple surfactant systems, micelles can form in either very polar or nonpolar solvents, but essentially no surfactant aggregation occurs in intermediate solvents such as alcohols and esters. This effect is related to the cohesive energy of the solvents usually measured by the Gordon parameter, which is defined as $\gamma/V^{1/3}$ (J/m^3), where γ is the surface tension and V is the molar volume.[34] As the solvent cohesive energy decreases, the driving force for aggregation also decreases. There is no evidence for amphiphile aggregation for solvents with a Gordon parameter below 1.3 J/m^3.[35] For water, the Gordon parameter is 2.75 J/m^3, and for alcohols it is around 0.6 J/m^3. Small amounts of water may change the Gordon parameter of solvents,[36] so we have made the solubility tests on binary mixtures of DNA−DTA and pure alcohols where the water content is too low to cause an effect. All of the alcohols used in this study (decanol, octanol, hexanol, butanol, and ethanol) are able to dissolve the DNA−DTA complex. The solubilization mechanism is likely associated with an alcohol-induced decrease in attractive interactions between the surfactant molecules, that is, with the destabilization of surfactant aggregates complexed with DNA. The solubility decreases as the alcohol chain length increases, and this is due to the fact that, as the chain length of the alcohol increases, the alcohol molecules act less as a solvent and more as a cosurfactant to the DNA−DTA aggregate. This issue will be further discussed later on. In Figure 2a are presented the SAXS spectra obtained for binary mixtures of DNA−DTA and alcohols at 40 wt %. The SAXS spectra, containing only one diffraction peak, become more structured, and the peaks get sharper with increasing alcohol chain length. The solution containing 40 wt % DNA−DTA is more fluid (disordered) for shorter alcohols; this reflects the increasing solubility of the DNA−DTA complex the shorter is the alcohol chain length. In Figure 2b is presented the temperature dependence of the first diffraction peak for the DNA−DTA/alcohol mixture also

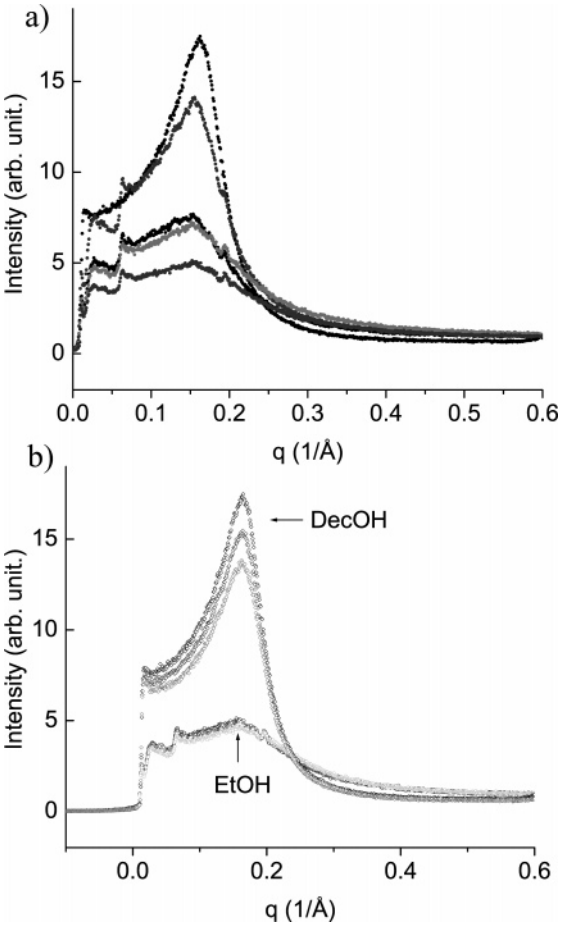

Figure 2. (a) SAXS spectra of the DNA−DTA/*n*-alcohol (DNA−DTA 40 wt %) solutions at 25 °C, area 1 in the phase diagrams; from bottom to top: ethanol, butanol, hexanol, octanol, and decanol. (b) SAXS spectra of DNA−DTA/decanol and DNA−DTA/ethanol (40 wt % DNA−DTA) solutions, area 1 in the phase diagrams, at different temperatures; from top to bottom: 25, 35, 45 °C.

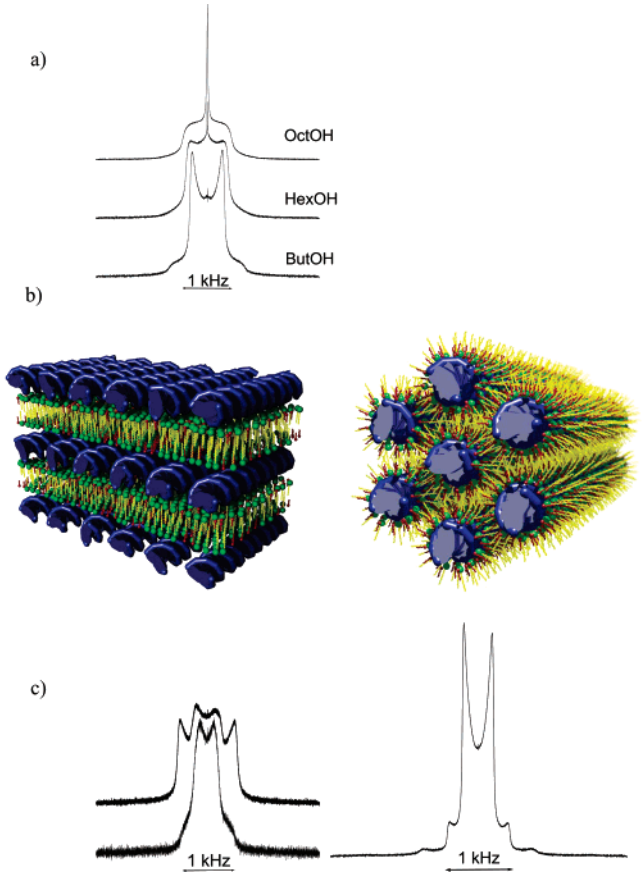

Figure 3. (a) ^{2}H NMR spectra for DNA−DTA/*n*-alcohol/water mixtures 30:40:30 wt %, area 4 in octanol and hexanol phase diagrams and area 19 in the butanol phase diagram. From bottom to top: butanol, hexanol, octanol. The LC area is wider for lower alcohols. (b) Schematic representation of the lamellar and reversed hexagonal phases obtained for DNA (blue)−DTA (green)/alcohol (red)/water mixtures. The alcohol molecules are incorporated within the aggregate to different degrees depending on the alcohol chain length. (c) ^{2}H NMR spectra for samples in area 19 in the DNA−DTA/butanol/water phase diagram. Left spectra: (top) 50:20:30 wt %; (bottom) 55:20:25 wt %. Right spectrum: 30:30:40 wt %. The double splitting corresponds to a lamellar phase coexisting with a hexagonal phase. The left side spectra are from samples on the same tie-line. The width of the splittings remains unchanged, but the relative intensity of the peaks is changing.

at 40 wt % of complex. In the case of decanol, the diffraction peak becomes less sharp as the temperature increases; the solution becomes more fluid and less ordered. We do not observe this effect for the ethanol case; at 40 wt % DNA−DTA in ethanol, the solution is fluid and disordered already at 25 °C. The fact that the SAXS peaks appear sharper for DNA−DTA solutions in longer alcohols could also be attributed to scattering contrast variations; however, it is macroscopically clear that the solubility of the complex decreases for lower alcohols. The temperature response shown in Figure 2b is a further indication that the DNA−DTA solutions of lower alcohols are more disordered. In addition, we can observe that the position of the first peak, indicating the characteristic distance between aggregates, shifts slightly to higher q values the higher is the alcohol chain, suggesting that the packing density of the aggregates at 40 wt % of DNA−DTA is higher for longer chain alcohols. In principle, by analyzing the SAXS spectra, one could obtain more structural information about this isotropic solution phase, the polydispersity and the shape of the aggregates; however, in this paper we will rather explore the phase behavior of the mixtures when water is added. Nevertheless, by studying the self-diffusion coefficient of the alcohol in the isotropic solution phase (results not shown here), we could see that the obstruction effect was far below the one obtained due to spherical aggregates. In these measurements, other complications arise because it is intricate to separate the effects of pure obstruction and/or interactions of the continuum alcohol phase with the aggregate. The structural properties of the DNA−DTA/alcohol binary mixture are not going to be further explored in this text; regarding this matter, it is sufficient to say that the difference of DNA−DTA solubility (and water) in the different alcohols will determine the extent of area 1 in all phase diagrams.

The Liquid Crystalline Region (Central Region in the Phase Diagrams). For all of the studied alcohols, the liquid crystalline region (LC) is located in the center of the phase diagram. The samples in this area have a solidlike morphology and show strong optical birefringence. In Figure 3a are presented the ^{2}H NMR spectra for samples with a DNA−DTA:alcohol:water composition of 30:40:30 wt %. The spectra consist of a mixture of the singlet expected for the isotropic aqueous phase and the splitting for the LC region. As the alcohol chain length is decreased, the intensity of the singlet is decreased, and for the case of butanol only the splitting can be observed. This is an indication that, as the alcohol chain length is decreased, more water is incorporated within the liquid crystalline DNA−DTA/alcohol aggregate. The central LC region is larger for lower alcohols. For the previously investigated decanol system, we

found that the nature of the LC phase in the central region of the phase diagram depended on the ratio between the volume fraction of DNA−DTA and the volume fraction of decanol. For higher amounts of decanol, a hexagonal phase was found, whereas for the low decanol side, the LC phase was of the lamellar type. Given that the hexagonal phase is obtained for the side with higher alcohol (long chain) content, it is reasonable to assume that it is of the reversed type.[14,19] In Figure 3b are schematically represented the LC lamellar and reversed hexagonal phases obtained for DNA−DTA/*n*-alcohol/water mixtures. The lamellar phase consists of a bilayer comprising surfactant and alcohol molecules intercalated with DNA molecules. This kind of structure was first suggested by Rädler et al. in a mixture of DNA and lipids.[13] The reversed hexagonal phase consists of DNA molecules decorated with surfactant molecules and alcohol.[14] The incorporation of alcohol molecules in the surfactant films is expected to be more efficient for alcohols with longer chain length.

For balanced amounts of water and decanol, these phases are separated by a two-phase region where the lamellar and the reversed hexagonal phases coexist. Essentially the same behavior as the lamellar phase in the water-rich side and the hexagonal phase in the alcohol-rich side is found for the different alcohols presented in this paper. The coexistence of the lamellar and hexagonal phases in the central LC area of the phase diagrams is clearly seen with quadrupolar splitting experiments. In Figure 3c are presented a few ^{2}H NMR spectra for samples in the LC coexistence region of the DNA−DTA/butanol/water system for different amounts of DNA−DTA. In all of the spectra, we can observe the double quadrupole splitting, indicating that two anisotropic liquid crystalline phases are in equilibrium. A larger splitting for the lamellar phase and a smaller one for the hexagonal phase, as well as the typical shoulders of the powder pattern spectrum,[37] can be resolved for a sample in the LC region (Figure 3c, right). In Figure 3c, left, are presented the spectra obtained for two samples with lower amounts of D_2O. The spectral resolution is worse, but the double splitting can still be observed. The splittings for the samples with less water (Figure 3c, left) are larger when compared to ones in the spectrum of the sample with more water (Figure 3c, right). An increase in the splitting magnitude is expected when the fraction of bonded ^2H_2O increases; reducing content water provides an environment less efficient with respect to averaging of the quadrupolar interactions, and higher splittings are obtained. An interesting finding confirming the correctness of the phase diagrams (Figure 1) is the fact that for samples belonging to the same tie-line (Figure 3c, left), we observe that the width of the splittings remains essentially unchanged as we move up on the tie-line (Figure 3c, left, from bottom to top) and the relative intensity of the peaks is changing. Qualitatively, we can observe that as we move up in the tie-line (area 19 in the butanol phase diagram), the intensity of the splitting for the lamellar phase is increasing.

The Hexagonal Phase Region. The SAXS spectra obtained for the different alcohols in the alcohol-rich corner are presented in Figure 4a. The relative positions of the Bragg peaks 1:$\sqrt{7}$ (decanol, octanol, hexanol) and 1:$\sqrt{3}$ (butanol, ethanol) confirm that the liquid crystalline phase for the alcohol-rich side is hexagonal. As the alcohol chain length is increased, we observe a shift to lower q values of the first diffraction peak. The characteristic distance given by the Bragg peak regards the unit cell dimensions containing DNA, surfactant, and alcohol molecules. The distance between the DNA rods decorated with surfactant molecules and alcohols will therefore increase as the chain length of the alcohol increases.

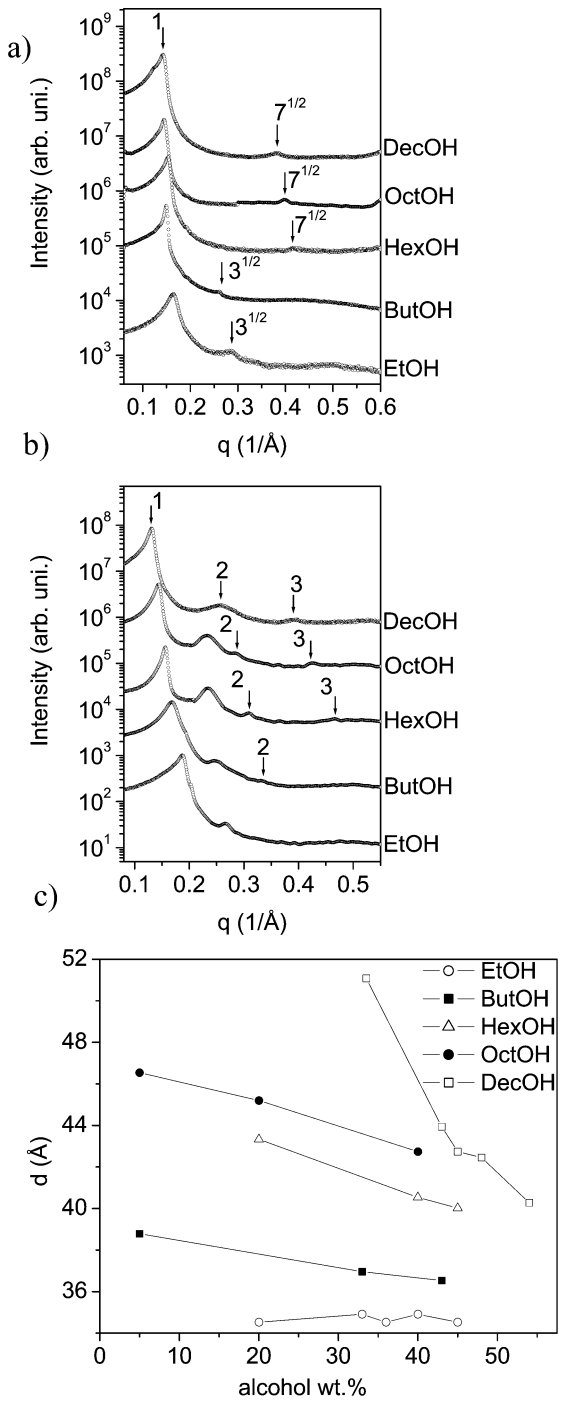

Figure 4. (a) SAXS diffraction patterns for samples in area 3 in the decanol, octanol, and hexanol phase diagrams and samples in area 1 in the butanol and ethanol phase diagrams. (b) SAXS diffraction pattern for samples in area 5 in the decanol, octanol, and hexanol phase diagrams and samples in area 17 and area 4 in the butanol and ethanol phase diagram, respectively. The hexagonal phase occurs for the alcohol-rich side in the phase diagrams, whereas the lamellar phase exists in the opposite part. (c) Interlayer spacing (Å) as a function of alcohol content. The spacing for ethanol remains constant, indicating a cosolvent effect; the other alcohols induce a decrease in spacing as alcohol content is increased; this indicates that the alcohol is a cosurfactant and is incorporated within the DNA−DTA aggregate.

The Lamellar Phase. The SAXS spectra obtained for samples with lower alcohol content are presented in Figure 4b. The liquid crystalline phase in this region is clearly a lamellar

phase. For decanol, three diffraction peaks can be resolved with relative positions of 1:2:3. As the alcohol chain length is decreased, the Bragg peaks are less clearly resolved, but an additional peak can be observed between the first and second peaks of the lamellar phase. This peak corresponds to the DNA−DNA repeat distance in the multilamellar phase of surfactants with intercalated DNA molecules aligned parallel to each other.[13] Similarly to what was found for the hexagonal phase, an increase in the lamellar repeat distance is found as the alcohol chain length increases. The distance between DNA rods is also increasing as the alcohol chain length is increasing. Longer chain alcohols are able to penetrate in the DNA−DTA aggregate. The presence of alcohol molecules in the surfactant film induces a dilution of the surfactant positive charges, causing them to be further apart. Because the DNA rods are in close contact with the positively charged surfactant molecules, a subsequent increase in DNA−DNA distance is expected.[14]

Alcohol molecules by themselves are not able to form an interface dividing hydrophobic and hydrophilic parts, but when mixed with longer chain surfactants (cosurfactant) they can induce effects on the surfactant structure. Lowering of interface rigidity is one example. Addition of hexanol in a molar ratio of 1:2 to an amphiphilic lamellar phase can decrease the elasticity energy from $20kT$ to $5kT$.[38]

To evaluate the role of cosolvent or cosurfactant of the different alcohols in the DNA−DTA aggregate, we studied the evolution of the interlayer spacing (d) as a function of alcohol content. In Figure 4c are presented the variations in the unit cell dimension (d) as the alcohol content is increased. For ethanol, no significant changes could be detected, but for the other alcohols the interlayer distance is decreasing as more alcohol is added; the effect is more pronounced for the decanol case. When the alcohol has a role as cosurfactant, penetrating into the surfactant core, increasing alcohol content leads to an increase in the area per surfactant hydrocarbon chain. For alcohols with shorter chain length than the surfactant, there is a decrease in the average hydrocarbon chain length of the aggregate.[38,39] If the alcohol acts as a cosolvent, no variations in the interlayer distance are expected, but when acting as cosurfactant, increasing alcohol content induces a reduction of the interlayer distance in both lamellar[14] and hexagonal[40] systems. In the DNA−DTA aggregate, ethanol seems to act as a cosolvent, whereas the other alcohols can be incorporated within the aggregate. In the surfactant world, the mixing of oil and water is associated with the formation of a microemulsion. In DNA-based surfactants, the films are too rigid so liquid crystalline phases are formed instead.[19] For all of the studied systems in this work, regardless of alcohol penetration in the DNA−surfactant film, always liquid crystalline phases were obtained.

Adding Salt to LC Phases. DNA interacts strongly with oppositely charged species via electrostatic interactions. With oppositely charged surfactants, the electrostatics drive the association while the hydrophobic interactions may govern what kind of supramolecular structure is stabilized. To investigate these two effects, we perturb the electrostatic forces in a lamellar and a hexagonal liquid crystalline phase of the DNA−DTA/decanol/water mixture by adding a 1:1 electrolyte (NaCl). In Figure 5 are presented the SAXS spectra obtained for samples with increasing salt content in the water component of the mixture. In Figure 5a, we can observe that as the salt content is increased in the lamellar phase, the first peak in the SAXS spectra is shifting to lower q values. DNA and surfactant molecules in the DNA−surfactant aggregate are separated by

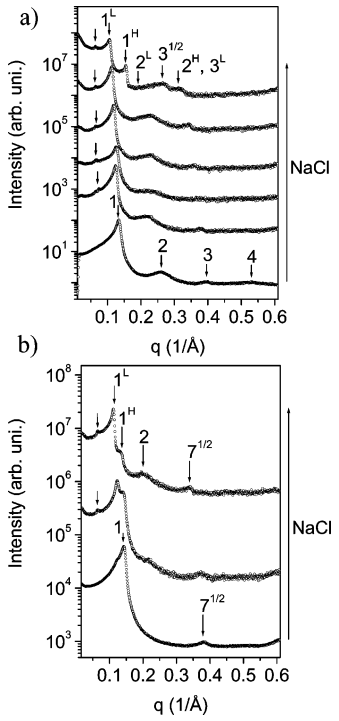

Figure 5. (a) SAXS diffraction patterns for samples in area 4b (lamellar LC phase) of the DNA−DTA/decanol/water phase diagram with increasing NaCl content in the water component. From bottom to top, the concentration of NaCl in M is 0, 0.001, 0.01, 0.5, 1, and 2. (b) SAXS diffraction patterns for samples in area 4a (hexagonal LC phase) in the DNA−DTA/decanol/water phase diagram with increasing NaCl content in the water phase. From bottom to top, the concentration of NaCl in M is 0, 0.001, and 0.5. The superscripts H and L in the peak assignments correspond to "hexagonal" and "lamellar", respectively. Increasing salt content induces an increase in the unit cell dimensions as well as the occurrence of mixed lamellar and hexagonal phases.

a thin layer of solvent. By adding salt into this solvent layer, the strong electrostatic attraction in the DNA−surfactant pair is screened.[41] As the salt content is increased from 0 to 1 mM, the repeat distance of the lamellar phase increases by 5 Å; this is an indication that the DNA−surfactant complex expands on the addition of salt due to screened electrostatic attractive interactions. Increases in unit cell dimension as the ionic strength is increased have been reported for DNA−polycation complexes[42] and other stoichiometric polyelectrolyte−surfactant complexes.[43] This observation reveals the importance of releasing the condensed polyelectrolyte and surfactant counterions during complex formation. In fact, this mechanism has been considered to be the main driving force for the aggregation of highly charged DNA and oppositely charged amphiphiles.[20] At higher ionic strengths, the entropic gain of counterion release upon complexation will be reduced relative to lower ionic strengths. In Figure 5, an additional peak of low intensity and low q value can also be observed as the salt content is increased; the corresponding characteristic distance is 99 Å. When the phase behavior of the system without DNA (DTAB/alcohols/water) was investigated by SAXS, we found that the lamellar phase of the mixed DTA/decanol/water for compositions equivalent to those in Figure 5a exists at a repeat distance of 100 Å. As the DTA content is increasing at constant alcohol content, the repeat distance of the lamellar phase decreases. The first peak observed in the SAXS spectra for lower q values could correspond to the lamellar phase of surfactant and decanol without DNA. This type of coexistence of pure amphiphilic phases with DNA−amphiphile phases has been observed for other DNA−lipid systems.[14] As the electrostatic attraction

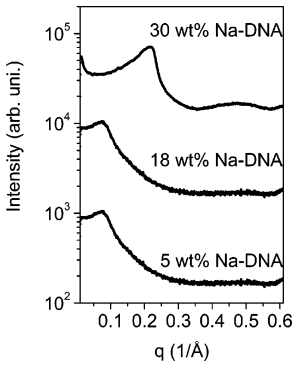

Figure 6. SAXS diffraction patterns for samples in the NaDNA/decanol/water mixture with increasing NaDNA content. From bottom to top, the compositions in wt % are 5:12:83, 18:12:70, and 30:12:58.

between the DNA and the surfactant molecules is screened, some surfactant molecules may abandon the complex and form another lamellar phase with decanol. For other polyelectrolyte−surfactant systems, it has been observed that when the salt content is much increased the complex is disassembled and there is a formation of solid surfactant precipitates.[43,44] This is an indication that addition of salt may induce departure of the surfactant molecules from the polyelectrolyte−surfactant complex. It could also be that there is an equilibration issue and that, given enough time, this demixing of surfactant molecules would eventually disappear. However, all samples were allowed to equilibrate at least 2 months before inspection.

Another observation is that, at high salt content, a hexagonal phase of shorter repeat distance than the lamellar phase starts to build up. At a very high ionic strength, there is evidence for the existence of two phases: lamellar and hexagonal. This effect is very common in surfactant systems; addition of salt reduces the repulsion between the headgroups of the surfactant molecules, allowing a closer packing. Adding salt to a lamellar phase of surfactant molecules generally induces a transition to a hexagonal phase of the reversed type. When DNA is present, there is, a priori, a large reduction of the electrostatic repulsion of surfactant headgroups now in close contact with the DNA phosphates. The formation of nonstoichiometric DNA−surfactant complexes due to surfactant departure at high salt content may change the conditions for packing constraints and spontaneous curvature of the surfactant molecules, which allows for the formation of other structures. It is difficult to extend the phase behavior of polyelectrolyte−surfactant complexes at moderate salt content to the situation of very high ionic strength,[43] as, for these conditions, scenarios of nonstoichiometric complexes[44] and charge reversal of the macromolecules due to overscreening[45] have been suggested. Another issue to consider is the possibility for the formation of condensed domains of DNA molecules[25] within the DNA−amphiphile aggregate. Hexagonal close packing of DNA has been observed in DNA−polycation complexes.[42] The hexagonal phase occurring at higher salt content in Figure 5a could arise from such a DNA packing; however, the reported unit cell dimensions of the DNA packing in DNA−polycation complexes are 10 Å smaller than the one observed for the hexagonal phase here. We investigated the phase behavior of NaDNA/decanol/water by SAXS with increasing DNA content. In Figure 6 are presented the SAXS spectra obtained for three samples; no hexagonal order could be clearly detected, and even if existing at the highest DNA content, it would have a repeat distance of roughly 30 Å. The hexagonal phase that appears here at high salt content has a repeat distance of roughly 40 Å. In Figure 5b is presented the evolution of the hexagonal phase of DNA−DTA/decanol/water as salt is added. Also here, as in the lamellar phase case, there is an increase in the spacing of the unit cell as the salt content is increased, as well as the appearance of lamellar and hexagonal phases at high salt content. A peak presumably arising from an aggregate composed of surfactant and decanol without DNA at 99 Å can also be observed. The departure of surfactant molecules from the complexes with increasing salt concentration and the consequent nonstoichiometry is probably the best explanation for a perturbation of packing constrains and surfactant spontaneous curvature, which allows for more than one LC phase to exist. Even if not totally understood, the fact that the addition of salt changes the phase behavior of DNA−amphiphile systems is an interesting observation; for instance, the efficiency of transfection of nonviral gene carriers has been directly linked to charge density and structure of the lipoplexes,[46] of which the systems discussed in this paper are analogues.

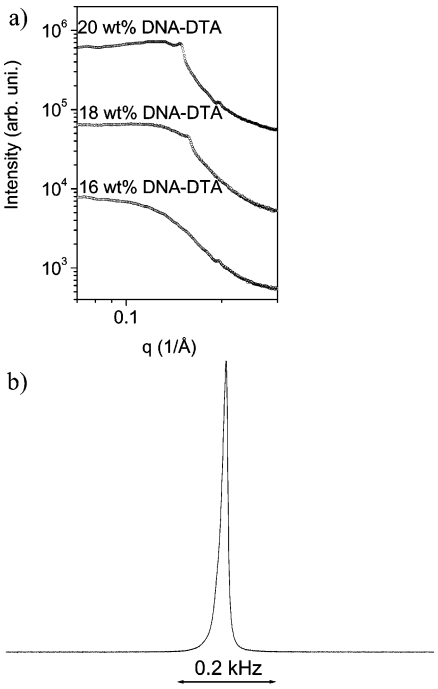

Figure 7. (a) SAXS diffraction patterns on log−log scale for samples in area S in the DNA−DTA/butanol/water phase diagram; the compositions in wt % from top to bottom are 20:48:32, 18:52:30, and 16:56:28. (b) ^{2}H NMR spectrum for a sample in area S in the DNA−DTA/butanol/water phase diagram of 18:52:30 wt %. The singlet indicates an isotropic nature of the S phase.

The Solution S Phase (Area 8 in Figure 1d). The study of phase behavior involving macromolecules can be rather intricate due to kinetic barriers that do not allow for complete equilibration of the system on a reasonable time scale. In this work, there was a waiting time of at least 2 months before inspection. Some of the samples were rechecked after half a year to clarify whether the same result was obtained. One of theses cases was the phase denoted as S (region 8) in the DNA−DTA/butanol/water phase diagram. The samples from this limited region are transparent and flow easily. They are optically isotropic but display birefringence, for instance, upon shear. The S phase is also very sensitive to temperature; heating from 25 to 35 °C leads to phase separation where the upper phase is an alcohol-like phase in equilibrium with a turbid bottom phase. The SAXS spectra for this region are presented in Figure 7a. At lower q, there is a plateau for higher dilution or a broad peak for higher DNA−DTA content. For these samples, the ^{2}H NMR spectra

consist of a singlet (Figure 7b), typically obtained for isotropic phases. For surfactant systems, the appearance of the so-called "sponge" or L3 phase is rather common.[47] The sponge phase has an intriguing surfactant bilayer arrangement, forming surfaces of zero or low mean curvature that separate different water channels and extend over macroscopic distances in three dimensions. This phase corresponds to a disordered version of a bicontinuous cubic phase and has isotropic properties; however, it can display flow birefringence.[48] The difference in free energy between the various bilayer structures is on the order of a small fraction of kT per molecule, which makes sponge phases rather sensitive to temperature or composition.[49] The L3 (sponge) phase has been studied with scattering techniques,[50,51] and, in general, depending on dilution, the SAXS spectra consist of a broad peak at low q, indicating lack of long-range order, followed by a $q^{-2}-q^{-4}$ decay behavior characteristic of the scattering from randomly oriented disks,[52] indicating a local lamellar structure. The phase region denoted by S in the DNA−DTA/butanol/water phase diagram seems to have many characteristics of sponge phases: it is a fluid transparent phase displaying flow birefringence, the ^{2}H NMR spectrum consists of a singlet typically obtained for isotropic phases, and the SAXS data indicate a lack of long-range order. In a log−log scale, there is no clear evidence for a linear decaying behavior with a q dependence of q^{-2}, which would suggest a local lamellar structure. The power of the q decay behavior is strongly affected by the solvent background, so a proper analysis of q dependence is only possible if the solvent background is removed.

We could picture the sponge phase with bilayers containing DTA and butanol interacting with DNA molecules randomly oriented in the water domains. Further work is required to clarify whether phase S is an equilibrium structure or not. The samples should be left to equilibrate for even longer times, and, for example, the SAXS data should be further investigated in terms of solvent background reduction. S is a very small phase region (as in fact are also L3 regions in simple surfactant systems) occurring for the DNA−DTA/butanol/water mixture that has the above presented characteristics after 6 months of equilibration.

Summary

The primary objective of this work was to investigate and understand the self-assembly behavior of a DNA−cationic surfactant complex in mixtures of *n*-alcohols and water. In the study of phase behavior, the components should be totally mixed and equilibrium achieved. The phase behavior study of the ternary mixture DNA−DTA/*n*-alcohols/water can be difficult because DNA is a high molecular weight polymer and equilibration occurs slowly. The mixture of the DNA−DTA complex with higher alcohols and water yields viscous solutions, and equilibrium takes a long time to be established. The binary mixtures of DNA−DTA and alcohols were investigated by SAXS; there is a reduced viscosity of the solutions for lower alcohols, and equilibrium is easier to achieve.

Different liquid crystalline phases are observed when water is added to DNA−DTA/*n*-alcohol solutions. The liquid crystalline region (LC) is located in the center of the phase diagrams, and the LC area becomes more extended for alcohols with shorter chain length. The samples in this area have a solidlike morphology and show strong optical birefringence. For higher *n*-alcohol contents, the liquid crystalline phase appears to be of the reversed hexagonal type for all of the studied systems. For the part with lower alcohol content, lamellar phases are encountered.

There is a coexistence of the two LC phases on the transition from the lamellar phase to the hexagonal phase. In this region, the ^{2}H NMR spectra display two splittings of different width, one for each LC phase. For samples on the same tie-line, the magnitudes of the splittings remain nearly unchanged, while the intensities of the peaks for the lamellar and the hexagonal splitting change; this is a good indication of the correctness of the phase diagram. We investigated the role of the alcohol as cosolvent or cosurfactant by measuring the variation of the interlayer distance as the alcohol content was added. Ethanol acts as a cosolvent, while higher alcohols function as cosurfactants. The effect of salt in the LC region was studied for the DNA−DTA/decanol/water system. Increasing the ionic strength in the water component of the mixture causes an increase in the unit cell dimensions of both the hexagonal and the lamellar phases. Adding salt loosens the DNA aggregate due to electrostatic screening. Furthermore, we observe the occurrence of mixed lamellar and hexagonal phases at high salt content.

When we go from the ternary mixtures with decanol, octanol, and hexanol to the DNA−DTA/butanol/water mixtures, major differences in the phase behavior start to arise. The phase diagram is more complicated, and there is an occurrence of a new phase denoted by S. This phase region is very small and has many characteristics of the disordered sponge (L3) phase often found in simple surfactant systems.

Acknowledgment. This work was supported by the Foundation for strategic research-SSF, The Swedish Institute, and The Swedish Research Council-VR. Part of this work was performed when B.L. was a visiting professor at the University of Coimbra with support from FCT grant no. PCTI/99/QUI/35415.

References and Notes

(1) Thalberg, K.; Lindman, B. Polymer−Surfactant Interactions-Recent Developments. In *Interactions of Surfactants with Polymers and Proteins*; Goddard, E. D., Ed.

(2) Robb, I. D. Polymer/Surfactant Interactions. In *Anionic Surfactants-Physical Chemistry of Surfactant Action*; Lucassen-Reynders, E., Ed.; Marcel Dekker: New York, 1981; p 109.

(3) Goddard, E. D. *Colloids Surf.* **1986**, *19*, 301.

(4) Saito, S. Polymer−Surfactant Interactions. In *Nonionic Surfactants*; Schick, M. J., Ed.; Marcel Dekker: New York, 1987; p 881.

(5) Hayakawa, K.; Kwak, J. C. T. *Interactions between Polymers and Cationic Surfactants*; Marcel Dekker: New York, 1991.

(6) Piculell, L.; Lindman, B. *Adv. Colloid Interface Sci.* **1992**, *41*, 149.

(7) Kwak, J. C. T. *Polymer−Surfactant Systems*; Marcel Dekker: New York, 1998.

(8) Svensson, A.; Piculell, L.; Cabane, B.; Ilekti, P. *J. Phys. Chem. B* **2002**, *106*, 1013.

(9) Zemb, T.; Dubois, M.; Deme, B.; Gulik-Krzywicki, T. *Science* **1999**, *283*, 816.

(10) Kaler, E. W.; Murthy, A. K.; Rodriguez, B. E.; Zasadzinski, J. A. N. *Science* **1989**, *245*, 1371.

(11) Minagawa, K.; Matsuzawa, Y.; Yoshikawa, K.; Khokhlov, A. R.; Doi, M. *Biopolymers* **1994**, *34*, 555.

(12) Yoshikawa, K.; Takahashi, M.; Vasilevskaya, V. V.; Khokhlov, A. R. *Phys. Rev. Lett.* **1996**, *76*, 3029.

(13) Rädler, J. O.; Koltover, I.; Salditt, T.; Safinya, C. R. *Science* **1997**, *275*, 810.

(14) Koltover, I.; Salditt, T.; Rädler, J. O.; Safinya, C. R. *Science* **1998**, *281*, 78.

(15) Barreleiro, P. C. A.; Olofsson, G.; Alexandridis, P. *J. Phys. Chem. B* **2000**, *104*, 7795.

(16) Hayakawa, K.; Santerre, J. P.; Kwak, J. C. T. *Biophys. Chem.* **1983**, *17*, 175.

(17) McManus, J. J.; Rädler, J. O.; Dawson, K. A. *Langmuir* **2003**, *19*, 9630.

(18) McManus, J. J.; Rädler, J. O.; Dawson, K. A. *J. Phys. Chem. B* **2003**, *107*, 9869.

(19) Bilalov, A.; Leal, C.; Lindman, B. *J. Phys. Chem. B* **2004**, *108*, 15408.

(20) Wagner, K.; Harries, D.; May, S.; Kahl, V.; Rädler, J. O.; Ben-Shaul, A. *Langmuir* **2000**, *16*, 303.

(21) Mel'nikov, S. M. *Langmuir* **1999**, *15*, 1923.
(22) Dias, R.; Mel'nikov, S.; Lindman, B.; Miguel, M. *Langmuir* **2000**, *16*, 9577.
(23) Leal, C.; Wadsö, L.; Olofsson, G.; Miguel, M.; Wennerström, H. *J. Phys. Chem. B* **2004**, *108*, 3044.
(24) Leal, C.; Topgaard, D.; Martin, R. W.; Wennerström, H. *J. Phys. Chem. B* **2004**, *108*, 15392.
(25) Livolant, F.; Leforestier, A. *Prog. Polym. Sci.* **1996**, *21*, 1115.
(26) Saenger, W. *Principles of Nucleic Acid Structure*; Springer-Verlag: New York, 1984.
(27) Persson, N. O.; Fontell, K.; Lindman, B.; Tiddy, G. J. T. *J. Colloid Interface Sci.* **1975**, *53*, 461.
(28) Wennerström, H.; Lindblom, G.; Lindman, B. *Chem. Scr.* **1974**, *6*, 97.
(29) Wennerström, H.; Persson, N. O.; Lindman, B. *Adv. Chem. Ser.* **1975**, *9*, 253.
(30) Stephenson, R.; Stuart, J.; Tabak, M. *J. Chem. Eng. Data* **1984**, *29*, 287.
(31) Stephenson, R.; Stuart, J. *J. Chem. Eng. Data* **1986**, *31*, 56.
(32) Sergeyev, V. G.; Pyshkina, O. A.; Lezov, A. V.; Mel'nikov, A. B.; Ryumtsev, E. I.; Zezin, A. B.; Kabanov, V. A. *Langmuir* **1999**, *15*, 4434.
(33) Sergeev, V. G. *J. Am. Chem. Soc.* **1999**, *121*, 1780.
(34) Evans, D. F.; Wennerström, H. *The Colloidal Domain: Where Physics, Biology and Technology Meet*; VCH: New York, 1998.
(35) Evans, D. F. *Langmuir* **1988**, *4*, 3.
(36) Graciani, M.; Muñoz, M.; Rodríguez, A.; Moyá, L. *Langmuir* **2005**, *21*, 3303.
(37) Davis, J. H. *Biochim. Biophys. Acta* **1983**, *737*, 117.
(38) Safinya, C. R.; Sirota, E. B.; Roux, D.; Smith, G. S. *Phys. Rev. Lett.* **1989**, *62*, 1134.
(39) Szleifer, I.; Kramer, D.; Ben-Shaul, A.; Roux, D.; Gelbart, W. M. *Phys. Rev. Lett.* **1988**, *60*, 1966.
(40) Aramaki, K.; Olsson, U.; Yamaguchi, Y.; Kunieda, H. *Langmuir* **1999**, *15*, 6226.
(41) Leal, C.; Moniri, E.; Pegado, L.; Wennertröm, H., to be submitted for publication.
(42) DeRouchey, J.; Netz, R. R.; Rädler, J. O. *Eur. Phys. J. E* **2005**, *16*, 17.
(43) Leonard, M. J.; Strey, H. H. *Macromolecules* **2003**, *36*, 9549.
(44) Thalberg, K.; Lindman, B.; Karlström, G. *J. Phys. Chem.* **1991**, *95*, 6004.
(45) Joanny, J. F. *Eur. Phys. J. B* **1999**, *9*, 117.
(46) Lin, A. J.; Slack, N. L.; Ahmad, A.; George, C. X.; Samuel, C. E.; Safinya, C. R. *Biophys. J.* **2003**, *84*, 3307−3316.
(47) Strey, R.; Schomäcker, R.; Roux, D.; Nallet, F.; Olsson, U. *J. Chem. Soc., Faraday Trans.* **1990**, *86*, 2253.
(48) Gomati, R.; Appel, J.; Bassereau, P.; Marignan, J.; Porte, G. *J. Phys. Chem.* **1987**, *91*, 6203.
(49) Wennerström, H.; Daicic, J.; Olsson, U.; Götz, J.; Schurtenberger, P. *J. Mol. Liq.* **1997**, *72*, 15.
(50) Maldonado, A.; Urbach, W.; Ober, R.; Langevin, D. *Phys. Rev. E* **1996**, *54*, 1774.
(51) Lei, N.; Safinya, C. R.; Roux, D.; Liang, K. S. *Phys. Rev. E* **1997**, *54*, 608.
(52) Schimidt, C. F.; Svoboda, K.; Lei, N.; Petsche, I.; Berman, L.; Safinya, C. R.; Grest, G. *Science* **1993**, *259*, 952.